Penta- and hexacoordinate silicon compounds with phosphorus donors [1]

Hans H. Karsch *, Roland Richter, Eva Witt

*Anorganisch-Chemisches Institut, Technische Universität München, Lichtenbergstr. 4, D-85747 Garching, Germany*

Abstract

The reaction of one or two equivalents of lithium phosphinomethanide $\{Li[C(PMe_2)_2(SiMe_2Ph)]\} \cdot$ TMEDA with p-TolSiCl$_3$ or $CH_2CH_2CH_2SiCl_2$ yields novel penta- and hexacoordinate silicon complexes. Both are the first examples of truly hypervalent organosilicon species with phosphorus donors to be characterized by X-ray diffraction studies. The crystal p-TolSiCl$_2[(PMe_2)_2C(SiMe_2Ph)]$ (1) adopts an intermediate state between a trigonal bipyramid and a tetragonal pyramid. Compound $CH_2CH_2CH_2Si[(PMe_2)_2C(SiMe_2Ph)]_2$ (2) is cis-hexacoordinated in solution and in the solid state, with comparable Si–P$_{ax}$ and Si–P$_{eq}$ bond lengths.

1. Introduction
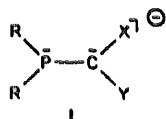
In monoanionic phosphinomethanides, I, the phosphorus and carbon atoms directly linked are isoelectronic with respect to their valence shells. Thus they have an ambiaent nature, in that they can react with electrophiles either via the carbon or the phosphorus atoms or both, the outcome depending on the nature of the metal and the substituents on phosphorus and carbon. In general, formation of metal–carbon bonds is preferred, but with an increasing number of heteroatom substituents (X, Y) on the carbanion center, formation of metal–phosphorus linkages is also possible. In particular, with *di*-phosphinomethanides (Y = PR$_2$), chelating or bridging P-coordination is often encountered, and further promoted in cases where X = PR$_2$, SiMe$_3$ [1]. Thus, high phosphine coordination numbers at metal centers are often achieved, even in cases where the metal center is very reluctant to accept phosphine coor-

dination, e.g. even with lanthanides [2]. This, in part, is due to the formation of four-membered chelate rings, which favor high coordination numbers.

With silicon as the electrophile, predominance of Si–C bond formation can be expected on thermodynamic grounds, but again, at least kinetically, Si–P bond formation also should be possible in cases where X, Y = PR$_2$ and/or SiMe$_3$. This is indeed observed, and phosphinomethanes and/or phosphorus ylides with heteroelement substituents are obtained in appropriate reactions [3]. In the case of *di*-phosphinomethanides these ylides are often fluxional in solution [4], and it has been concluded that higher coordination numbers at silicon in the transition state are responsible for a rapid exchange of phosphino groups in solution, as depicted in II.
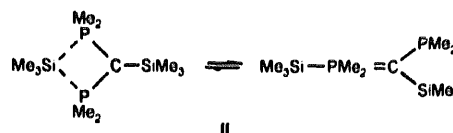
Hypervalency in organosilicon chemistry now is a quite common and well-understood phenomenon, mainly driven forward in recent years by Corriu and coworkers [5]. Electronegative ligands (F, Cl, O, N) are usually present at the silicon center. Therefore, in order to

convert the hypervalent transition state of type **II** into a ground state, it seemed logical to replace the organic substituents at silicon, at least in part, by more electronegative ones, e.g. chlorine.

In fact, even hexacoordination is achieved in the system $SiCl_4$–$Li[C(PMe_2)_2(SiMe_3)]$ [6], whereas in the system Me_2SiCl_2–$Li[C(PMe_2)_2(SiMe_3)]$ [7], 'true' hexacoordination is only observed in solution; in the solid state, only weak Si–P_{eq} interactions contribute to a framework on the borderline between tetrahedral and (distorted) octahedral.

Pentacoordination at silicon with phosphorus donor ligands has not yet been observed in the solid state, but for $PhSiCl_3$–$Li[C(PMe_2)_2(SiMe_3)]$ a pentacoordinated species was recently detected spectroscopically in solution [4].

In the present paper, we describe: (a) the preparation and structure of the first phosphorus donor complex of a pentacoordinate organosilicon center to be characterized by an X-ray diffraction study; (b) the preparation and structure of the first phosphorus donor complex of an organosilicon center which is 'truely' hexacoordinated, both in solution and in the solid state.

2. Results

2.1. Synthesis of p-TolSiCl₂[(PMe₂)₂C(SiMe₂Ph)] (1)

With the objective of obtaining a crystalline complex with pentacoordinate silicon, to achieve a better crystallinity compared with that of $PhSiCl_2[(PMe_2)_2$ $C(SiMe_3)]$, the phenyl group was replaced by a p-tolyl and the SiMe₃ by an SiMe₂Ph group.

Treatment of p-TolSiCl₃ with {Li[C(PMe₂)₂ (SiMe₂Ph)]} · TMEDA in an ethereal solvent led to isolation of the monosubstitution product. p-

$TolSiCl_2[(PMe_2)_2C(SiMe_2Ph)]$ is obtained as a colorless crystalline solid.

$$p\text{-TolSiCl}_3 + \{Li[C(PMe_2)_2(SiMe_2Ph)]\} \cdot TMEDA \longrightarrow p\text{-Tol}-\underset{\underset{Me_2P=\!=\!=}{\overset{Cl}{|}}{Si}} \quad (1)$$
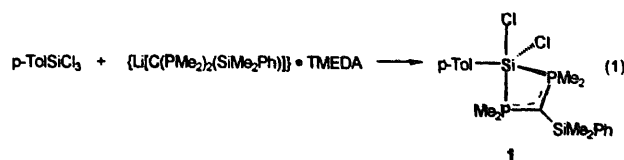
The presence of only one single resonance (a singlet) in the $^{31}P\{^1H\}$ NMR spectrum of **1** at ambient temperature ($\delta^{31}P = 39.08$) and $-100°C$ ($\delta^{31}P = 39.33$) indicates a rapid equilibration process of the phosphino groups. The singlet resonance is accompanied by silicon satellites ($^1J(PSi) = 77.3$ Hz), which is matched by a triplet signal from the central silicon nucleus in the $^{29}Si\{^1H\}$ NMR spectrum. Pentacoordination is also indicated by the high field shift of this nucleus ($\delta^{29}Si = -75.98$). The ^1H and ^{13}C NMR spectra of **1** are in full accord with the observed structure, which was confirmed by an X-ray diffraction study.

2.2. Structure of p-TolSiCl₂[(PMe₂)₂C(SiMe₂Ph)](1)

$p\text{-TolSiCl}_2[(PMe_2)_2C(SiMe_2Ph)]$ crystallizes in the space group $P\bar{1}$ with two molecules in the unit cell. In the solid state (Figs. 1(a) and 1(b); Table 1), the molecule adopts a geometry at the central Si(1) atom, that can be described as intermediate between a trigonal bipyramid (tbp) and a tetragonal pyramid. The deviation from the tbp-geometry is evident from the (comparatively) large Cl(2)–Si(1)–P(2) angle (134.58°) and the small Cl(1)–Si(1)–P(1) angle (158.64(4)°) and is caused by the very small 'bite-angle' (69.82(3)°) of the diphosphinomethanide ligand (P(1) ⋯ P(2) nonbonding distance is 2.697 Å). Furthermore, P(1) shows a large thermal deflection in the direction of a tetragonal pyramid. This

Table 1
Bond lengths (Å) and angles (deg) for 1

|			
Cl(1)–Si(1)	2.1904(8)	Cl(2)–Si(1)	2.1113(8)
P(1)–C(1)	1.730(2)	P(1)–C'(12)	1.809(4)
P(1)–C(11)	1.820(4)	P(1)–Si(1)	2.4070(9)
P(1)–P(2)	2.6973(9)	P(2)–C(1)	1.718(2)
P(2)–C(22)	1.805(3)	P(2)–C(21)	1.809(3)
P(2)–Si(1)	2.3036(8)	Si(1)–C(101)	1.859(2)
Si(2)–C(1)	1.827(2)	Si(2)–C(202)	1.867(3)
Si(2)–C(201)	1.870(2)	Si(2)–C(203)	1.883(2)
C(1)–P(1)–Si(1)	90.78(7)	C(1)–P(2)–Si(1)	94.66(8)
C(101)–Si(1)–Cl(2)	111.08(8)	C(101)–Si(1)–Cl(1)	100.93(7)
Cl(2)–Si(1)–Cl(1)	92.63(3)	C(101)–Si(1)–P(2)	112.34(7)
Cl(2)–Si(1)–P(2)	134.58(4)	Cl(1)–Si(1)–P(2)	91.76(3)
C(101)–Si(1)–P(1)	96.22(7)	Cl(2)–Si(1)–P(1)	92.98(3)
Cl(1)–Si(1)–P(1)	158.64(4)	P(2)–Si(1)–P(1)	69.82(3)
C(1)–Si(2)–C(203)	110.3(1)	C(202)–Si(2)–C(203)	108.5(1)
C(201)–Si(2)–C(203)	107.3(1)	P(2)–C(1)–P(1)	103.0(1)
P(2)–C(1)–Si(2)	130.5(1)	P(1)–C(1)–Si(2)	126.5(1)

(a)

(b)
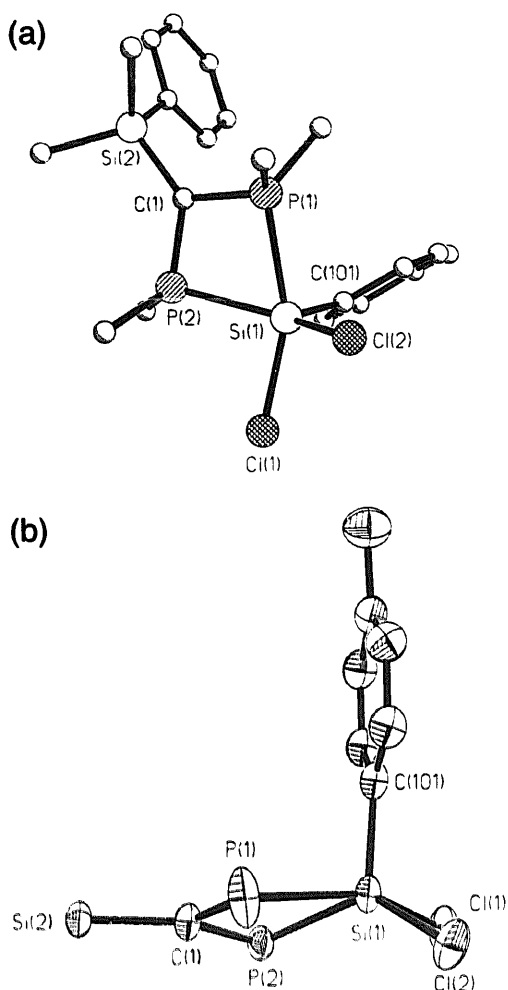
Fig. 1. (a) Molecular structure of **1** (H atoms omitted, ball and stick model); (b) molecular skeleton of the structure **1** (plot along with displacement ellipsoids).

arrangement of the two phosphorus atoms facilitates rapid equilibration of the two phosphorus donors, as indicated by the ^{31}P{^{1}H} NMR spectrum. In comparison

with 'equatorial' bond distances in tbp-structures, the 'axial' distances are usually longer by ca. 8%. Both, the Si–P and the Si–Cl bond lengths show deviations in the expected direction: the Si(1)–P(2) bond length is ca. 0.1 Å shorter than Si(1)–P(1) (Si(1)–Cl(1) = 2.1904(8) Å, Si(1)–Cl(2) = 2.1113(8) Å). The P–C(1) bonds of the dihapto-coordinated ligand are within the usual range, and can be attributed to the partial ylidic character of these bonds and the different Si–P bond lengths.

2.3. Synthesis of $\overline{CH_2CH_2CH_2Si}[(PMe_2)_2C(SiMe_2Ph)]_2$ (2)

The aim of obtaining better stabilization of an octahedral environment at silicon compared with that in $Me_2Si[(PMe_2)_2C(SiMe_3)]_2$ was achieved by replacing the Me_2Si moiety by a silacyclobutane moiety. As before, the $SiMe_3$ group of the ligand was replaced by an $SiMe_2Ph$ group to give better crystallinity.

Two equivalents of $\{Li[C(PMe_2)_2(SiMe_2Ph)]\}$ · TMEDA reacted with $\overline{CH_2CH_2CH_2SiCl_2}$ in diethyl ether to give **2** as a colorless, crystalline solid.
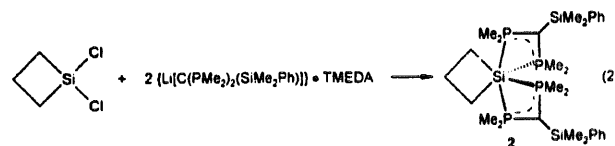
The ^{31}P{^{1}H} NMR spectrum of **2** shows a broad singlet at ambient temperature. Cooling to $-60°C$ establishes an AA'BB'-spin system, as expected for the cis-isomer. The weighted chemical shift is essentially temperature-independent and rules out dissociative processes in solution. In contrast to $Me_2Si[(PMe_2)_2C(SiMe_3)]_2$, which decomposes in solution in a few days at room temperature [8], compound **2** shows a high thermal stability;

Table 2
Bond lengths (Å) and angles (deg) for **2**

P(1)–C(1)	1.745(2)	P(1)–C(11)	1.829(2)
P(1)–C(12)	1.835(2)	P(1)–Si(1)	2.4807(6)
P(2)–C(1)	1.732(2)	P(2)–C(22)	1.826(2)
P(2)–C(21)	1.827(2)	P(2)–Si(1)	2.3739(5)
Si(1)–C(2)	1.931(2)	Si(2)–C(1)	1.829(2)
Si(2)–C(201)	1.865(2)	Si(2)–C(202)	1.877(2)
Si(2)–C(203)	1.883(2)	C(2)–C(3)	1.540(3)
C(11)–P(1)–C(12)	99.8(1)	C(22)–P(2)–C(21)	99.3(1)
C(2)–Si(1)–C(2)'	77.3(1)	C(2)–Si(1)–P(2)'	100.37(6)
C(2)–Si(1)–P(2)	98.96(6)	P(2)'–Si(1)–P(2)	155.18(4)
C(2)–Si(1)–P(1)'	166.30(6)	C(2)'–Si(1)–P(1)'	96.30(6)
C(2)–Si(1)–P(1)	96.30(6)	P(2)–Si(1)–P(1)'	94.08(2)
C(2)'–Si(1)–P(1)	166.30(6)	P(2)–Si(1)–P(1)	63.36(2)
P(1)'–Si(1)–P(1)	92.39(3)	P(2)–C(1)–P(1)	103.42(9)
P(2)–C(1)–Si(2)	128.7(1)	P(1)–C(1)–Si(2)	127.6(1)
C(3)–C(2)–Si(1)	89.8(1)	C(2)'–C(3)–C(2)	103.1(2)

heating **2** for 4 weeks (80°C) leaves it unchanged except for the appearance of a small amount of $HC(PMe_2)_2(SiMe_2Ph)$ produced by hydrolysis [3].

2.4. Structure of $\overline{CH_2CH_2CH_2Si[(PMe_2)_2C(SiMe_2Ph)]_2}$ (2)

Compound **2** crystallizes in the monoclinic space group $C2/c$ with four molecules lying on a two-fold rotation axis in the unit cell. The molecular structure (Fig. 2; Table 2) of **2** shows three planar four-membered ring systems (sum of the angles in each case 360.0°), one involving the silacyclobutane moiety and two arising from the chelating diphosphinomethanide ligands. The difference between the $Si-P_{ax}$ and $Si-P_{eq}$ bond lengths (2.374(1)/2.481(1) Å) is within the expected range in view of the respective trans influences, and clearly distinguishes this 'true' hexacoordination from the case of $Me_2Si[(PMe_2)_2C(SiMe_3)]_2$ ($Si-P_{ax}$: 2.300/2.306 Å; $Si-P_{eq}$: 2.868/2.962 Å) [7]. The dihedral angle between the plane $C(2)-Si(1)-C(2)'$ and the plane through $P(2)-Si(1)-P(2)'$ is 89°. The dihedral angle of 17° between the silacyclobutane plane and the plane through $P(1)-Si(1)-P(1)'$ indicates the deviation from an ideal octahedral geometry. The small $P(2)-Si(1)-P(2)'$ angle of 155° is a consequense of the ring
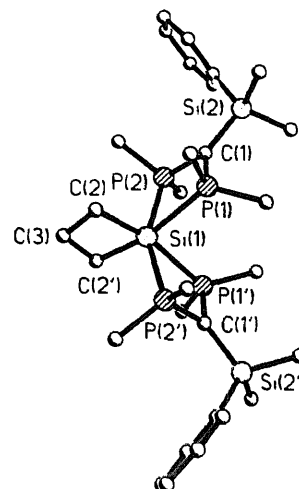
strain within the four-membered rings with a ligand bite angle of 68.4°, which also results in a small $P(1) \cdots P(2)$ nonbonding distance of 2.729 Å. As in **2**, the $P-C(1)$ distances within the ligand framework are shortened due to their particular ylidic character. The $Si-C$ bonds of the silacyclobutane ring distances are slightly elongated, and allow a small $C(2)-Si(1)-C(2)'$ angle of 77.3°.

Fig. 2. Molecular structure of **2** (H atoms omitted, ball and stick model).

Table 3
Crystallographic data for **1** and **2**

	$C_{20}H_{30}Cl_2P_2Si_2$	$C_{29}H_{52}P_4Si_3$
Molecular formula		
Molecular mass (g mol^{-1})	459.461	608.861
Crystal system	Triclinic	Monoclinic
Space group	$P\bar{1}$	$C2/c$
d_{calc} (g cm^{-1})	1.233	1.181
a (Å)	9.762(1)	16.469(2)
b (Å)	10.847(1)	9.186(1)
c (Å)	12.284(1)	24.740(2)
α (deg)	77.85(1)	90
β (deg)	77.00(1)	113.78(1)
γ (deg)	89.61(1)	90
V (Å^3)	1237.9(2)	3425.0(6)
Z	2	4
μ (mm^{-1})	0.492	0.343
Crystal dimensions (mm^3)	$0.60 \times 0.35 \times 0.15$	$0.50 \times 0.40 \times 0.35$
Data collection diffractometer	CAD4	CAD4
Radiation	Mo Kα, graphite monochromator	Mo Kα, graphite monochromator
2Θ range (deg)	6-52	6-50
Reciprocal space	$-11 \leq h \leq 12$,	$-18 \leq h \leq 19$,
	$-13 \leq k \leq 13$,	$0 \leq k \leq 10$,
	$0 \leq l \leq 15$	$-29 \leq l \leq 5$
Scan mode	$\omega - \Theta$	$\omega - \Theta$
Independent reflections	4829	3724
Observed reflections	3896	2613
Program	SHELXL-93	SHELXL-93
Parameters	242	167
R ^{a}/$wR2$ ^{b} ($F_0 > 4\sigma F_0$)	0.0378/0.0915	0.0281/0.0762
R ^{a}/$wR2$ ^{b} (all reflections)	0.0545/0.1001	0.0347/0.0802

^{a} $R = \Sigma||F_0| - |F_c||/\Sigma|F_0|$; ^{b} $wR2 = \{\Sigma w(|F_0| - |F_c|)^2/\Sigma w(F_0)^2\}^{1/2}$.

Table 4
Atomic coordinates and equivalent isotropic displacement parameters ($\AA^2 \times 10^3$) for 1

	x	y	z	U_{eq} [a]
Cl(1)	0.21902(7)	0.55642(5)	0.05411(5)	0.0450(2)
Cl(2)	0.35502(7)	0.47663(6)	0.26303(6)	0.0457(2)
P(1)	0.26116(9)	0.18085(6)	0.23430.0(6)	0.0477(2)
P(2)	0.23674(6)	0.25681(5)	0.06611(5)	0.0313(1)
Si(1)	0.21357(7)	0.39008(5)	0.19189(5)	0.0293(2)
Si(2)	0.22200(7)	-0.04379(5)	0.16322(5)	0.0292(2)
C(1)	0.2405(2)	0.1223(2)	0.1681(2)	0.0293(4)
C(11)	0.1446(5)	0.0969(3)	0.4162(3)	0.092(2)
C(12)	0.4328(5)	0.1578(4)	0.3163(5)	0.121(2)
C(21)	0.3924(4)	0.2985(3)	-0.0485(3)	0.069(1)
C(22)	0.0999(3)	0.2562(3)	-0.0111(2)	0.0505(7)
C(101)	0.0297(2)	0.3904(2)	0.2760(2)	0.0321(5)
C(102)	0.0014(3)	0.3769(2)	0.3948(2)	0.0382(5)
C(103)	-0.1348(3)	0.3671(2)	0.4592(2)	0.0413(6)
C(104)	-0.2489(3)	0.3693(2)	0.4087(2)	0.0380(5)
C(105)	-0.2211(3)	0.3852(2)	0.2905(2)	0.0404(5)
C(106)	-0.0848(3)	0.3967(2)	0.2252(2)	0.0360(5)
C(107)	-0.3966(3)	0.3541(3)	0.4806(3)	0.0563(7)
C(201)	0.3390(3)	-0.1414(2)	0.2455(2)	0.0431(6)
C(202)	0.2676(3)	-0.0677(2)	0.0133(2)	0.0468(6)
C(203)	0.0358(2)	-0.1055(2)	0.2309(2)	0.0328(5)
C(204)	-0.0756(3)	-0.0264(3)	0.2447(2)	0.0454(6)
C(205)	-0.2132(3)	-0.0741(3)	0.2900(3)	0.0618(8)
C(206)	-0.2400(3)	-0.2028(3)	0.3241(2)	0.0616(9)
C(207)	-0.1322(4)	-0.2824(3)	0.3139(2)	0.0567(8)
C(208)	0.0038(3)	-0.2357(2)	0.2670(2)	0.0428(6)

[a] U_{eq} is defined as one-third of the trace of the orthogonalized U_{ij} tensor.

3. Experimental part

3.1. Preparation of p-TolSiCl₂[(PMe₂)₂C(SiMe₂Ph)], 1

0.99 ml (5.61 mmol) of p-TolSiCl₃ was added to a solution of 1.55 g (1.87 mmol) of {Li[C(PMe₂)₂(SiMe₂Ph)]}₃ and 0.84 ml (5.61 mmol) of TMEDA in 30 ml of diethyl ether at −78°C. After warming up to room temperature a white suspension was formed, which was stirred for 12 h. The solvent was replaced by pentane and, after filtration and evaporation of the pentane, a colorless, crystalline solid of 1 (2.23 g; 86.4%), melting point 78°C, remained.

Anal. Found.: C, 50.34; H, 6.93. C₂₀H₃₀Cl₂P₂Si₂

Table 5
Atomic coordinates and equivalent isotropic displacement parameters ($\AA^2 \times 10^3$) for 2

	x	y	z	U_{eq} [a]
P(1)	-0.07589(3)	0.21975(5)	0.17396(2)	0.0239(1)
P(2)	0.08177(3)	0.08835(5)	0.19257(2)	0.0256(1)
Si(1)	0.0000	0.03282(7)	0.2500	0.0232(2)
Si(2)	0.02248(3)	0.34099(5)	0.09458(2)	0.0288(1)
C(1)	0.0092(1)	0.2193(2)	0.14894(7)	0.0254(4)
C(2)	-0.0668(1)	-0.1314(2)	0.20531(8)	0.0355(4)
C(3)	0.0000	-0.2356(3)	0.2500	0.0483(8)
C(11)	-0.1815(1)	0.1579(2)	0.11739(8)	0.0381(4)
C(12)	0.1013(1)	-0.0636(2)	0.15167(9)	0.0397(5)
C(22)	0.1960(1)	0.1500(3)	0.23229(9)	0.0425(5)
C(201)	-0.0864(2)	0.3856(3)	0.03374(9)	0.0489(6)
C(202)	0.0751(1)	0.5186(2)	0.1283(1)	0.0573(7)
C(203)	0.095(1)	0.2510(2)	0.06215(7)	0.0279(4)
C(204)	0.1875(1)	0.2608(2)	0.08882(8)	0.0370(4)
C(205)	0.2410(1)	0.1821(3)	0.06822(9)	0.0451(5)
C(206)	0.2032(1)	0.0936(3)	0.01962(9)	0.0447(5)
C(207)	0.1121(1)	0.0840(2)	-0.00866(9)	0.0413(5)
C(208)	.0595(1)	0.1623(2)	0.01248(8)	0.0336(4)

[a] U_{eq} is defined as one-third of the trace of the orthogonalized U_{ij} tensor.

(459.48). Calc.: C, 52.28; H, 6.53%. ^{31}P{^{1}H} NMR (270 MHz; C_6D_6; 25°C): $\delta P = 39.08$ (s; Si-satellites: ^1J(PSi) = 78.5 Hz). ^{31}P{^{1}H} NMR (270 MHz; Toluol-d_8; –100°C): $\delta P = 39.33$ (s). ^{29}Si{^{1}H} NMR (400 MHz; C_6D_6; 25°C): $\delta Si = -12.32$ (t; ^2J(PSi) = 4.7 Hz; SiMe$_2$Ph); –75.98 (t; ^1J(PSi) = 77.3 Hz; Si$_{central}$). ^{1}H NMR (270 MHz; C_6D_6; 25°C): $\delta H = 8.17–6.79$ (Ar; 9H); 1.12 (t; $N = 9.3$ Hz; PMe$_2$; 12H); 0.23 (s; SiMe$_2$; 6H).

3.2. Preparation of $\overline{CH_2CH_2CH_2Si[(PMe_2)_2C(SiMe_2-Ph)]_2}$, 2

0.17 ml (1.43 mmol) of $\overline{CH_2CH_2CH_2SiCl_2}$ was added to a solution of 0.79 g (0.95 mmol) of {Li[C(PMe$_2$)$_2$(SiMe$_2$Ph)]}$_3$ and 0.43 ml (2.86 mmol) of TMEDA in 30 ml of diethyl ether at –78°C. After warming up to room temperature a white suspension was formed, which was stirred for 12 h. The solvent was replaced by pentane and, after filtration and evaporation of the pentane, a colorless, crystalline solid of 3 (0.82 g; 94.7%), melting point 111°C, remained.

Anal. Found: C, 56.50; H, 8.86. $C_{29}H_{52}P_4Si_3$ (608.86). Calc.: C, 57.21; H, 8.54%. ^{31}P{^{1}H} NMR (270 MHz; Toluol-d_8; 25°C): $\delta P = 26.70$ (brs). ^{31}P{^{1}H} NMR (270 MHz; Toluol-d_8; –60°C): $\delta P = 29.92$ (m, $P_{A/A'}$); 25.51 (m, $P_{B/B'}$); J(AA') = $\pm$125 Hz; J(BB') = J(AB') = J(A'B) = $\pm$250 Hz; J(AB) = J(A'B') = $\pm$590 Hz. ^{29}Si{^{1}H} NMR (270 MHz; C_6D_6; 25°C): $\delta Si = -10.94$ (s, SiMe$_2$Ph); = 146.99 (s, Si$_{central}$). ^{13}C{^{1}H} NMR (270 MHz; C_6D_6; 25°C): $\delta C = 143.96$ (s; C$_1$); 134.48 (s; $C_{2/6}$); 128.53 (s; C$_4$); 127.72 (s; $C_{3/5}$); 35.32 (quint; ^2J(PC) = 31.9 Hz; CH$_2$CH$_2$CH$_2$); 20.21 (br; PMe$_2$); 13.80 (s; CH$_2$CH$_2$CH$_2$); 2.67 (s; SiMe$_2$). ^{1}H NMR (270 MHz; C_6D_6; 25°C): $\delta H = 7.58$ (m; Ar; 4H); 7.17 (m; Ar; 6H); 1.80 (br; CH$_2$CH$_2$CH$_2$ not resolved; 6H); 1.08 (br; PMe$_2$; 24H); 0.37 (s; SiMe$_2$; 12H).

3.3. Crystal structure analysis of 1 and 2

Crystallographic measurements were made at 205 K (1) and 211 K (2) with graphite-monochromated Mo K α radiation ($\lambda = 0.71073$ Å) on an Enraf–Nonius CAD4-Turbo diffractometer (Tables 3, 4 and 5). The crystals

used for measurement were colorless plates of sizes 0.60 mm × 0.35 mm × 0.15 mm (1) and 0.50 mm × 0.40 mm × 0.35 mm (2). For 1 and 2, the unit-cell dimensions (Table 3) were determined by 100 reflections of high diffraction angles using values between $\theta = 9°$ and 13°. The intensity data were measured by continuous $\omega–\theta$ scans. Measured data were corrected for Lorentz and polarization effects [9]. The structures were solved by direct methods. Refinement was done by the full-matrix least squares method. All calculations were performed using SHELXL-93 [10]. In the structural models, all non-hydrogen atoms were assigned anisotropic displacement parameters. The coordinates of the hydrogen atoms were geometrically calculated and refined using the a 'riding model'. Tables of H atom coordinates and thermal parameters and a complete list of bond lengths and angles have been deposited at the Fachinformationszentrum Karlsruhe, Gesellschaft für wissenschaftlich-technische Informationen m.b.H., D-76344 Eggenstein-Leopoldshafen, under the following numbers: CSD 404920 (1) and CSD 404921 (2).

References

[1] H.H. Karsch, Russ. Chem. Bull., 42 (1993) 1937.

[2] H.H. Karsch, G. Ferazin, H. Kooijman, O. Steigelmann, A. Schier, P. Bissinger and W. Hiller, J. Organomet. Chem., 482 (1994) 151.

[3] H.H. Karsch, R. Richter, B. Deubelly, A. Schier, M. Paul, M. Heckel, K. Angermaier and W. Hiller, Z. Naturforsch. Teil B., 49 (1994) 1798.

[4] H.H. Karsch, R. Richter and A. Schier, Z. Naturforsch. Teil B., 48 (1993) 1533.

[5] (a) C. Chuit, R.J.P. Corriu, C. Reyé and J.C. Young, Chem. Rev., 93 (1993) 1371; (b) C. Brelière, F. Carré, R.J.P. Corriu and G. Royo, Organometallics, 7 (1988) 1006; (c) F. Carré, C. Chuit, R.J.P. Corriu, A. Mehdi and C. Reyé, Angew. Chem., 106 (1994) 1152.

[6] H.H. Karsch, B. Deubelly, U. Keller and G. Müller, Chem. Ber., in press.

[7] H.H. Karsch, B. Deubelly, U. Keller, F. Bienlein, R. Richter and G. Müller, Chem. Ber., in press.

[8] R. Richter, Thesis, TU München, 1996.

[9] A. Kopf and H.-C. Rubke, Program CADSHEL, Version 3.10, University of Hamburg, 1993.

[10] G.M. Sheldrick, Program SHELXL-93, University of Göttingen, 1993.